Characteristics of Multitube Multishroud Supersonic Jet Noise Suppressor

H. T. NAGAMATSU,* R. E. SHEER JR.,† AND M. S. GILL‡
General Electric Research and Development Center, Schenectady, N.Y.

A supersonic jet noise suppressor with 191 tubes and 191 hexagonal shrouds was investigated at jet Mach numbers of 1.4 and 0.71. Flow and acoustic data were obtained for the plain jet and various suppressor configurations. With 191 tubes the sonic location was decreased from 19 in. for an equivalent $1\frac{9}{16}$-in.-diam. jet to approximately 1 in. The jets coalesced at approximately $1\frac{1}{2}$ in. and the Mach number was 0.73, with an over-all sound power level reduction of 15.2 db from the plain jet and a thrust loss of 10.2%. By adding 6.0-in. multishrouds to the tubes, the over-all sound power level reduction was 20.4 db. The impact pressure fluctuations decreased as x^{-2} downstream of the peak location for all configurations. The calculated thrust loss for the tubes and 6 in. multishrouds was 20.8% and the measured loss was 26.7%. Multitubes with the 6.0 in. multishrouds decreased the sound power level by 9.4 db for a Mach 0.71 jet.

Introduction

A JET exhaust noise suppression research program is being conducted at the General Electric Research and Development Center. Sound suppressors of various configurations were investigated to suppress the sound and understand the noise generation mechanisms of supersonic jets. Some of the results of the previous experimental and analytical investigations were presented in Refs. 1–3.

It was observed previously that supersonic jet exhaust noise can be decreased most effectively by making the supersonic flow sonic in the shortest possible distance from the nozzle exit. The techniques used to reduce the jet exhaust velocity are shock waves, induced flow, and division of flow through multiple exits as discussed in the above references. It was observed in Ref. 3 that the length of the supersonic region was related to the Mach number and the exit diameter. This method of using multiple exits to decrease velocity was used quite successfully in Refs. 4 and 5.

In order to improve upon the previous supersonic jet exhaust sound suppressors, a series of tests was conducted on multitube and new multishroud suppressors and an attempt was made to correlate the flow and acoustic characteristics. This paper presents the results of these investigations. The effects of the length of the multishrouds and the location of the shroud leading edge from the tube exits were determined. Comparison is made with the equivalent $1\frac{9}{16}$-in.-diam convergent nozzle, and the acoustic data was analyzed by means of the supersonic jet noise theory of Nagamatsu and Horvay.[3] The over-all sound power level reduction and the percentage thrust loss for various multishroud configurations were determined.

Equipment and Procedure

The jet exhaust noise test facility consists of a 4-in.-diam pipe supplying air to a 12 in. diam by 24 in. long plenum chamber which is located 6 ft above the ground and 60 ft away from the building. The nozzle or the tube bundle can be attached at the end of the plenum chamber. The compressed air for the jet flow is provided by an 800 hp compressor.

A $1\frac{9}{16}$-in.-diam convergent nozzle is attached to the plenum chamber. The nozzle was used to compare its acoustic, flow, and thrust measurements with those of the various types of multitube and multishroud suppressors.

The tube bundle consists of 191 tubes with an outside diameter of 0.125 in., inside diameter of 0.115 in., and length of 2 in. The tubes are soldered into a $3\frac{3}{4}$-in.-diam plate. The ratio of the base area of the tube bundle to the internal area of the tubes is 4.72. The air is supplied to the tubes through the adaptor that is mounted to the plenum chamber in place of the $1\frac{9}{16}$-in.-diam convergent nozzle, Fig. 1.

The 191 multishrouds are made of hexagonal aluminum honeycomb material that provides a separate shroud for each tube of the 191 tube bundle, cf. Fig. 1. The over-all length of the shrouds are 1.667, 3.335, and 6 in. with each side of the hexagonal element equal to 0.155 in. The multishrouds can be easily slipped over each individual tube, and the opening between the base of the multitubes and the entrance to the multishrouds can be varied.

The S_{12}' shroud is made up of a 5 in. long by $5\frac{1}{2}$-in. inside diameter bellmouth adaptor fastened to a 7 in. long pipe with an inside diameter of 4 in. The $S_{3.8}$ shroud is a 3.795 in. long and 3.795-in. inside diameter cylinder open at both ends. It is tapered at the leading edge and has a diameter of 4.241 in. there, as shown in Fig. 1. Like all other shrouds, their main purpose is to

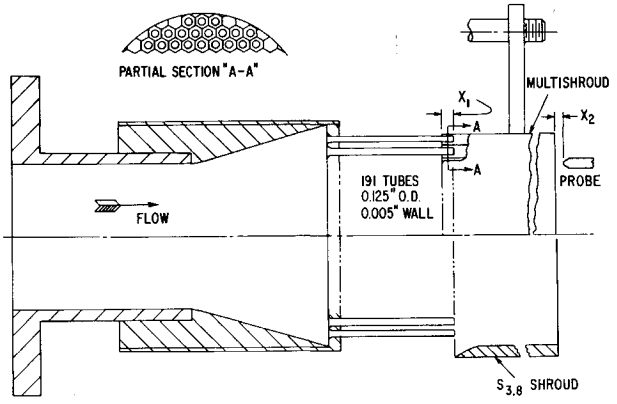

Fig 1 Sketch of multitube suppressor and shrouds.

Presented as Paper 71-153 at the AIAA 9th Aerospace Sciences Meeting, New York, January 25–27, 1971; submitted February 5, 1971; revision received October 6, 1971. This work was supported in part by the Federal Aviation Administration, through the Flight Propulsion Division, Evendale.

Index categories: Aerodynamic and Powerplant Noise (Including Sonic Boom); Jets, Wakes, and Viscid-Inviscid Flow Interactions; Supersonic and Hypersonic Flow.

* Research Associate. Fellow AIAA.
† Fluid Mechanics Engineer. Member AIAA.
‡ Mechanical Engineer.

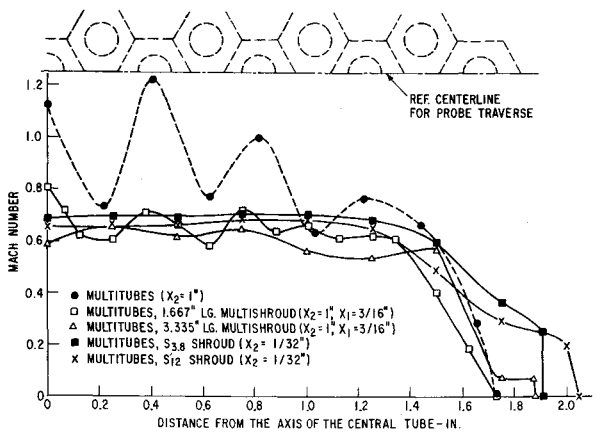

Fig. 2 Mach number profile across exits of multitubes, multishrouds, and single shrouds.

induce secondary flow and provide good mixing between the induced and the primary flows.

The sound was tape recorded at eight stations on the plane of the axis of the nozzle or the tube bundle by a $\frac{1}{2}$-in.-diam B & K microphone, and a GRC Type 1525 tape recorder. These stations were located on an arc of 10 ft radius extending from the exit of the configurations at angles of 19.1°, 33.6°, 43.8°, 60°, 80.4°, 99.6°, 120°, and 146.4° from the jet axis. The tape recordings were analyzed with a B & K $\frac{1}{3}$ octave band analyzer to determine the over-all sound pressure levels, over-all sound power levels, $\frac{1}{3}$ octave sound power spectra, and directivities.[6] In addition to the tape recordings, sound was also measured with a B & K sound level meter and a Ballantine RMS voltmeter.

Radial impact pressure and total temperature surveys of the flow near the exits of the various suppressor configurations were obtained at several axial locations. The axial surveys were made with impact pressure, total temperature, and piezoelectric probes. The probes were mounted on the trolley and traverses were made from the jet exit to the 80 in. location. The probe to measure the axial variation of the local total pressure fluctuations inside the jet consists of a Kistler $\frac{1}{4}$-in.-diam quartz piezoelectric pressure transducer having a response time of approximately 20 μsec. It is thus possible to measure high-frequency impact pressure fluctuations within the jet. The output from the pressure transducer was recorded with a Ballantine RMS voltmeter.

Flow Characteristics

Investigations were made at a reservoir to ambient pressure ratio of 3.2 with a room temperature air supply. Based on the isentropic expansion, a pressure ratio of 3.2 corresponds to a jet Mach number of 1.4. Radial impact pressure and total temperature surveys were made for various configurations. Using these measurements, the calculated Mach number profiles for multitubes with and without shrouds are presented in Fig. 2. x_2 in this paper refers to the distance of the probe leading edge from the jet exit and x_1 refers to the distance of the shroud leading edge upstream of the tube exit, cf. Fig. 1. Because of the large velocity gradients between the primary and induced flows close to the exits, surveys for the multitubes and multitubes with multishrouds were made at $x_2 = 1$ in. The Mach number profile for the multitubes is still quite nonuniform because the jets are still coalescing as shown in Ref. 7. The higher velocities occur in front of the tubes whereas the lower velocities occur in between them. For multitubes at the axis of the central tube of the tube bundle the Mach number is 1.12. The Mach number at 0.22 in. radial location is 0.73. At the 0.4 in. location, the probe is in the center of the tube and thus a higher Mach number is observed. The difference in Mach number due to the probe location becomes smaller at the 1.03, 1.22, and 1.43 in. location. This could be due to the fact that near the outer section of the tube bundle, more flow is being induced and the mixing tends to make the flow more uniform. This greater amount of induced flow also makes the velocity lower towards the outer edge and it becomes zero at the 1.73 in. location.

For the 1.667-in.-long multishrouds the flow is more uniform than for the multitubes but there is still an appreciable difference between the velocities measured at different locations as indicated in Fig. 2. The Mach number distribution for the 3.335-in.-long multishrouds is quite uniform from the centerline to the 1.5 in. location and beyond that there is an abrupt decrease until it becomes zero at a distance of about 1.85 in. from the axis. The uniformity of the flow is due to the better mixing of the primary and induced flows in the longer length of the multishrouds.

The Mach number distribution for the $S_{3.8}$ and the S_{12}' shroud is practically uniform from the axis to the 1.25 in. location. The average Mach number for these shrouds is higher than that for the multishrouds. This is due to the fact that the surveys were made $\frac{1}{32}$ in. downstream of the exit of these shrouds and 1 in. downstream of the exit of the multishrouds. Because of the larger exit area and larger induced flow through the bellmouth inlet, the curve for the S_{12}' shroud is lower than that for the $S_{3.8}$ shroud. The Mach number for the $S_{3.8}$ shroud decreases rather sharply between the 1.25 and 1.9 in. location and becomes zero at approximately 1.91 in. For the S_{12}' shroud, the Mach number decreases more gradually beyond the 1.25 in. location and becomes zero at approximately 2.05 in.

Figure 3 shows the radial Mach number profiles downstream of the exits of the multitubes and multishrouds for different values of x_1 and x_2. For the multitubes it is seen that the flow is more nonuniform closer to the exit. Mixing of the primary and secondary flows will tend to make the flow more uniform at a greater distance downstream of the tube exits. The general trend of the curves for $x_2 = \frac{1}{2}$ in. and $x_2 = 1$ in. is almost the same. Both curves indicate lower velocities near the periphery due to the greater mixing with the ambient air as mentioned previously. With no induced flow, $x_1 = 2$ in., and $x_2 = \frac{1}{2}$ in., the velocity is lower than that of multishrouds with induced flow and $x_2 = 1$ in. The lower velocity is due to the stronger shocks at the exit of the tubes without the induced flow. A similar observation was also made in Ref. 2 with a larger diameter shroud.

Axial impact pressure and total temperature surveys were made for the multitubes with and without multishrouds. Using these measurements, the axial Mach number distributions were calculated and are plotted in Fig. 4. At the $\frac{1}{16}$ in. location, the Mach number for the multitubes is 1.37. The Mach number decreases to 0.96 at approximately the $\frac{1}{2}$ in. location and 0.73 at 1.5 in. From 1.5 to 15 in. the Mach number remains almost constant like a subsonic jet. There is a marked difference in the flow pattern between that from the tube bundle and from the equivalent area nozzle. This is largely due to the entrained flow through the tube spacings that slows down the primary flow. However, after the 40 in. location, the velocity decay is the same for both the curves.

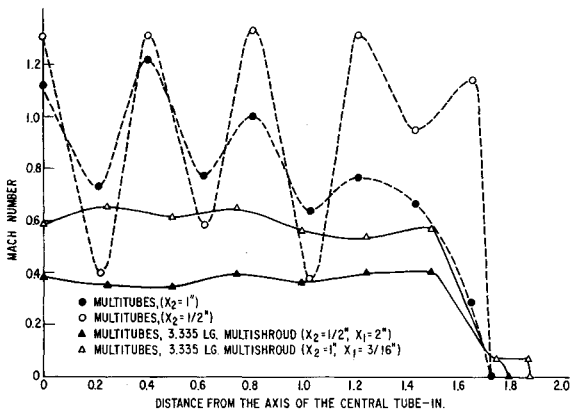

Fig. 3 Mach number profile across exits of multitubes and multishrouds.

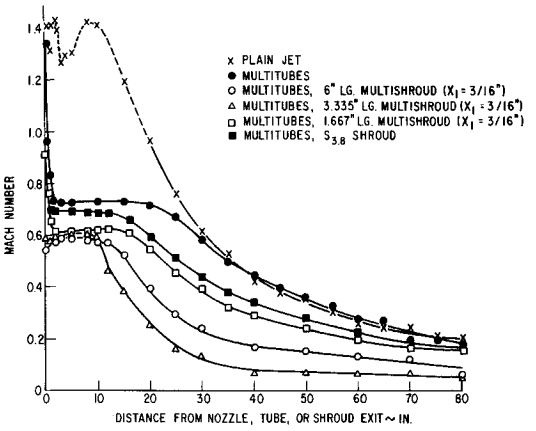

Fig. 4 Axial Mach number variation for multitubes with and without shrouds.

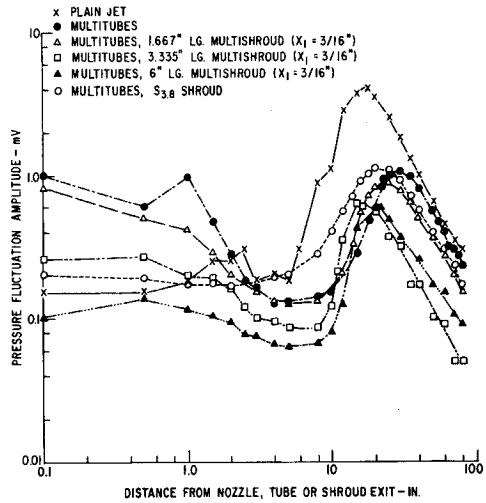

Fig. 6 Axial impact pressure fluctuations for multitubes with and without shrouds.

With multitubes, shock diamonds were observed over the initial 1 in. from the tube exit and this indicates that the flow is supersonic there, but Fig. 4 indicates only subsonic flow. The reason being that the probe was oscillating slightly and for these small diameter tubes, instead of recording the flow velocity at the center of the tube it was recording the velocity of the mixture of primary and induced flow. As can be seen from Fig. 2, the flow is quite nonuniform near the tube exit.

With the addition of the 1.667 in. long multishrouds at $x_1 = \frac{3}{16}$ in., the Mach number at the exit is 0.9 and becomes 0.6 at the 2 in. location and varied very little from 2 to 16 in., Fig. 4. Downstream of this location the velocity decayed gradually. In the region of constant Mach number, there is a difference of approximately 0.1 Mach number between the multitubes and the 1.667 in. long multishrouds.

For the 3.335-in.-long multishrouds at $x_1 = \frac{3}{16}$, the Mach number at the exit is 0.59 and remains fairly constant until the 10 in. location, then decreases rather sharply between 10 and 30 in. Further downstream the velocity decay is very gradual. Between 2 and 8 in., the Mach number is nearly the same for both the 1.667-in. and 3.335-in.-long multishrouds. The lowest Mach number of 0.54 occurs at the exit for the 6-in.-long multishrouds.

For the $S_{3.8}$ shroud the Mach number at the exit is 0.69 and stays almost constant for the initial 12 in. as indicated in Fig. 4. The velocity decay for $S_{3.8}$ is quite similar to the 1.667 in. long multishrouds and is lower than that of the multitubes.

Figure 5 presents the axial Mach number distribution for multitubes with multishrouds for various locations of the shroud leading edge from the exit of the multitubes. For $x_1 = 2$ in. and no induced flow, the flow becomes subsonic a short distance downstream of the tube exits as shown in Ref. 2. Because of the shock waves, the flow slows down faster than the flow through the shrouds with induced flow. The length of the shroud from the tube exits to the shroud exits for the 3.335-in.-long multishrouds with $x_1 = 2$ in. and the 1.667-in.-long multishrouds with $x = \frac{3}{16}$ in. is almost the same but the velocities are respectively 540 fps and 950 fps. The velocity for the 3.335-in.-long multishrouds with $x_1 = 2$ in. decreases from 540 fps at the exit to 400 fps at the 1.5 in. location. It varies very little over 1.5 to 10 in. and then decreases steadily from 10 to 35 in.

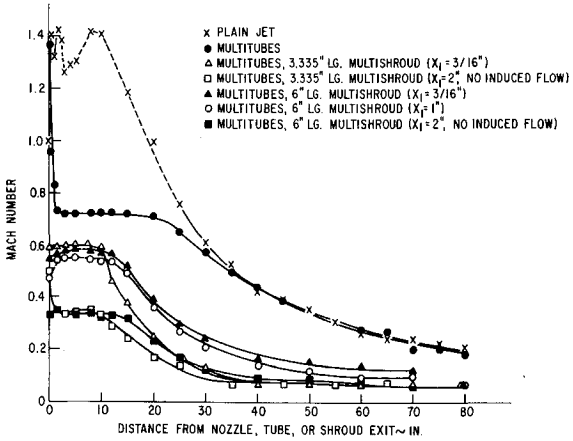

Fig. 5 Axial Mach number for multishrouds with varying location of shroud leading edge from exits of multitubes.

For the 6-in.-long multishroud with $x_1 = 1$ in., the velocity at the exit is lower than that for $x_1 = \frac{3}{16}$ in. The trend of velocity decay is quite similar for these two curves. For the 6-in.-long multishrouds with $x_1 = 2$ in. and no induced flow, the velocity at the exit is about 380 fps. It stays constant for about 12 in. before beginning to decrease.

The axial impact pressure fluctuations for multitubes with and without the multishrouds for $x_1 = \frac{3}{16}$ in. is presented in Fig. 6. These amplitudes are presented in terms of rms values in millivolts. For the plain nozzle, the impact pressure fluctuations at 0.1 in. from the exit is 0.15 mv and it remains low until the 5 in. location. The curve then rises rapidly and reaches the highest value of 4 mv at 18 in. and then decreases steadily. The peak fluctuations occur at $x/D = 11.5$. From Fig. 4 it is noticed that sonic conditions on the axis exist at $x/D = 12.1$. The peak or maximum pressure fluctuation thus occurs just ahead of the sonic point as observed previously in Refs. 2 and 7.

For multitubes, the fluctuations at 0.1 in. and at 1.0 in. is 1.0 mv, Fig. 6. It attains the lowest value of 0.13 mv at the 5 in. location and then reaches the highest value of slightly over 1 mv at the 30 in. location. The first peak at 1.0 in. occurs near the sonic point, cf. Fig. 4. A short distance beyond, the jets from the tubes start mixing with the entrained flow, and it then behaves like a subsonic jet of $3\frac{1}{2}$ in. diam. The peak occurs at approximately 9 of these diameters. This location is the same as that observed in Ref. 7 for subsonic jets where the peak pressure fluctuations occur at the end of the primary region of mixing between the jet and the ambient air. This region corresponds to the adjustment region as defined by Lighthill.[8]

For the 1.667-in.-long multishrouds the peak occurs at 25 in. at a value of 0.85 mv. In this case there is only one peak as compared to two with the multitubes. The trend of the curves for the multishrouds of various length is the same. The peak for the 3.335-in.-long multishroud occurs at 15 in. whereas for the 6 in. the peak is at 20 in., which agrees with the more rapid velocity decay for the shorter shroud, Fig. 4. The shape of the curve for the $S_{3.8}$ shroud is different from that of the other curves, the fluctuations decreased gradually from the exit to the 2 in. position

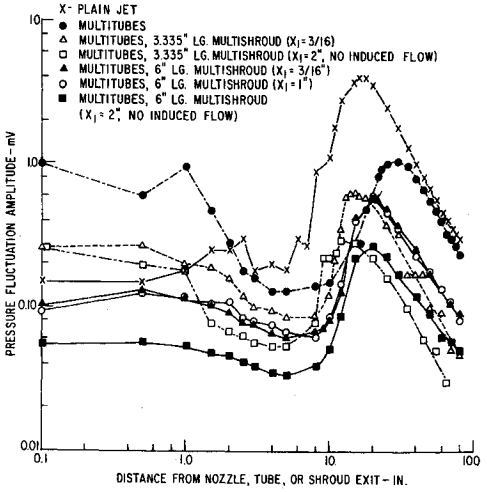

Fig. 7 Axial impact pressure fluctuations for multishrouds with varying location of shroud leading edge from exits of multitubes.

and begin to increase for greater distances with the peak fluctuations occurring at the 20 in. locaton. The maximum fluctuation is higher than all other configurations except the plain jet. However, the fluctuation decay is quite similar to all other configurations.

The pressure fluctuations for the multishrouds with varying location of the shroud leading edge from the exits of the multitubes are presented in Fig. 7. The general trend of curves for the 3.335-in. multishrouds at $x_1 = \frac{3}{16}$ in. and 2 in., no induced flow, is quite similar but the peak fluctuations at $x_1 = \frac{3}{16}$ in. is appreciably higher than that for $x_1 = 2$ in. Very little difference is noticed between the curves for $x_1 = \frac{3}{16}$ in. and $x_1 = 1$ in. for the 6-in. multishroud. With this shroud the curve for $x_1 = 2$ in. indicates the lowest fluctuations of all configurations over the initial 18 in. from the exits.

Thrust Loss

For the various configurations that were investigated, the change in thrust from the equivalent convergent nozzle was measured with the delta-thrust device described in Ref. 9. and is presented in Table 1. The change in thrust from the plain nozzle is due to the skin friction in the 191 tubes and 191 shrouds and to the base drag of the tube holder. An analysis was made in Ref. 9 to calculate the friction drag for the tubes and shrouds from the observed flow conditions and to determine the base drag from the measured base pressure distributions. The results from these calculations are also presented in Table 1.

Acoustic Characteristics

The sound pressure level for the multitube and multishroud suppressor configurations is plotted in Fig. 8 as a function of the angular position from the jet axis. The plain jet has its highest

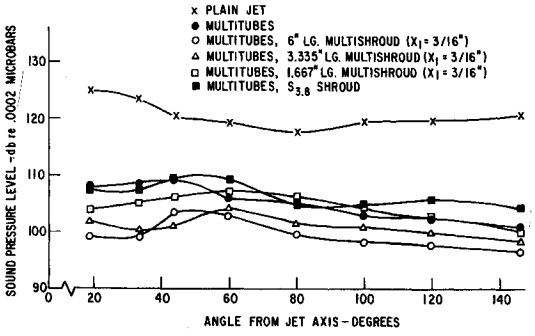

Fig. 8 Over-all sound pressure level as a function of angular position from jet axis for multitubes with and without shrouds.

Table 1 Thrust loss due to base drag, 191 tubes and 191 shrouds skin friction

Configuration	Base drag $\Delta T/T$%	Skin friction: Tubes $\Delta T/T$%	Skin friction: Shrouds $\Delta T/T$%	Total $\Delta T/T$%	Exp $\Delta T/T$%
Tubes	−2.00	−7.18		−9.18	−10.2
Tubes, 1.667 in.-long shrouds ($x_1 = \frac{3}{16}$ in.)	−4.98	−7.18	−5.87	−18.03	−6.8
Tubes, 3.335-in.-long shrouds ($x_1 = \frac{3}{16}$ in.)	−4.41	−7.18	−8.62	−20.2	−26.7
Tubes, 6-in.-long shrouds ($x_1 = \frac{3}{16}$ in.)	−2.11	−7.18	−11.5	−20.8	−26.7

level at the 19.1° location and its lowest at 80°. The sound pressure level for the multitubes at the 19.1° position is 108 db and increases to a maximum value of about 109 db at 43.8°. It then decreases continuously to the lowest value of 101 db at the 146.4° location.

At the 19.1° location the curve for the 6-in. multishrouds at $x_1 = \frac{3}{16}$ in. indicates 99 db and has a maximum value of about 103 db at the 43.8° location. At higher angles, the curve decreases steadily. This configuration shows the lowest over-all sound power level of all the suppressors that were investigated. The curve for the 3.335-in.-long multishrouds is slightly higher than the 6-in. multishrouds and the general trend of both curves is the same, but the 1.667 in. multishrouds is different. This curve rises continuously from 19.1° to 60° and then decreases at the higher angles. At most of the angular positions, the sound pressure level for the $S_{3.8}$ shroud is higher than the others.

The sound pressure levels for the S_{12}' shroud and for the 6-in. multishrouds with varying location of the shroud leading edge from the exits of the multitubes are presented in Fig. 10. At all positions, the sound pressure levels for $x_1 = 1$ in. are higher than that of $x_1 = \frac{3}{16}$ in. For $x_1 = 2$ in., no induced flow, the curve indicates even higher levels than those for $x_1 = 1$ in. between 30° and 70° but lower values beyond that. At the 146.4° position, the 6 in. multishrouds with no induced flow has caused a reduction of about 35 db from the plain jet. The curve for the S_{12}' shroud follows the multitubes curve quite closely and at no point is there a difference of more than 2 db between them. The maximum sound pressure level for S_{12}' shroud occurs at 60° whereas for all others it occurs at 43.8°.

The sound power spectra for the suppressor configurations, described in Fig. 8, for a frequency range of 40–16,000 Hz, is presented in Fig. 9. The maximum sound power level of 144.5 db

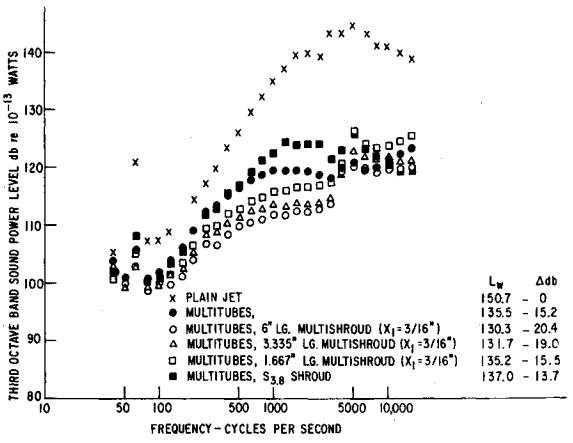

Fig. 9 Sound power level spectra for multitubes with and without shrouds.

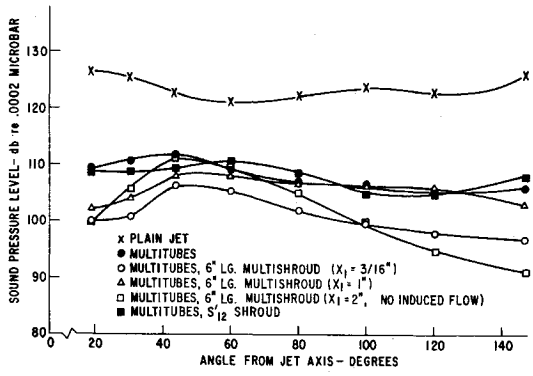

Fig. 10 Over-all sound pressure level as a function of angular position from the jet axis for S_{12}' shroud and for multishrouds with varying location of shroud leading edge from exits of multitubes.

occurs at 5000 Hz for the $1\frac{9}{16}$-in.-diam convergent nozzle. At higher frequencies it decreases continuously and at 16,000 Hz it is 138.5 db. For multitubes, the sound power level increases continuously from 75 to 1000 Hz and attains a value of 119.5 db. The sound power level stays almost constant to 6300 Hz before starting to rise at higher frequencies. The over-all sound power level for multitubes is 135.5 db, which is a reduction of 15.2 db from the plain jet for an outside air temperature of 68°F. A further reduction of 5.2 db is achieved with the 6 in. multishrouds at $x_1 = \frac{3}{16}$ in. Throughout the entire frequency range, except between 4000 and 6300 Hz, the sound power level for the 6 in. multishrouds is lower than any other configuration. Like all the other suppressors, the variation in power levels between 1000 Hz and 3200 Hz is very small. There is an abrupt increase between 3200 Hz and 4000 Hz. A maximum value of 120.5 db occurs at 5000 Hz and becomes 119 db at 8000 Hz. The curve rises very gradually for the higher frequencies.

The curve for the 3.335-in. multishrouds at $x_1 = \frac{3}{16}$ in. is very similar to that of the 6-in. multishrouds. At all frequencies, the sound power level for the 3.335 in. is higher than that for the 6-in. multishrouds. The 3.335 in. multishrouds reduces the power level by 19.0 db from the plain jet, which is only 1.4 db less than the 6-in. suppressor. The power spectra for the 1.667 in. multishrouds at $x_1 = \frac{3}{16}$ in. is higher but very similar to those for the 6 in. and 3.335 in. From 40 to 400 Hz, the sound power levels with the $S_{3.8}$ shroud and the 191 tubes is almost the same and beyond it starts to increase for the $S_{3.8}$ shroud. The $S_{3.8}$ shroud attains the maximum value of 126 db at 5000 Hz. This configuration has actually increased the sound power level from that of the multitubes.

Sound power spectra for the configurations of Fig. 10 are presented in Fig. 11. Below 5000 Hz, the sound power levels for

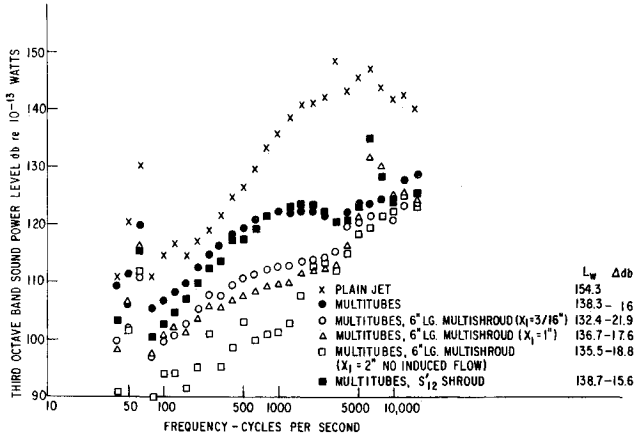

Fig. 11 Sound power level spectra for S_{12}' shroud and multishroud with varying location of shroud leading edge from exits of multitubes.

the 6-in. multishrouds at $x_1 = 1$ in. are lower than that for $x_1 = \frac{3}{16}$ in. The level increases sharply for $x_1 = 1$ in. at frequencies higher than 5000 Hz. At 6300 Hz the sound power level for $x_1 = 1$ in. has a peak of 131.5 db and decreases to 124 db at 16,000 Hz. From 40 to 1600 Hz, the level for the 6-in. multishrouds at $x_1 = 2$ in. is considerably lower than any other configuration but at higher frequencies it does not have any definite trend. The curve for the S_{12}' shroud seems to be close to the curve for multitubes. In this figure the S_{12}' shroud is the least effective suppressor for a jet Mach number of 1.4. It has increased the sound power level by 0.4 db from that of tubes alone.

In order to obtain some information regarding the effectiveness of supersonic jet noise suppressors at typical jet engine conditions, the $1\frac{9}{16}$-in.-diam convergent nozzle and the multitubes with the 6-in.-long multishrouds were operated at a pressure ratio of 1.4 with a corresponding jet Mach number of 0.71. For this pressure ratio the over-all sound power level was 9.4 db less than the plain jet, Table 2. Thus, the multitube multishroud suppressor obtains a significant noise reduction even for a subsonic jet Mach number of 0.71.

A convergent nozzle was used as a reference to determine the reduction in the over-all sound power levels, Table 2, for various combinations of multitubes and multishrouds. The area for this nozzle was equivalent to the total area of 191 tubes.

The supersonic jet noise theory of Nagamatsu and Horvay[3] was used to analyze the acoustic results for the plain jet and multitubes. With this theory it is possible to determine the acoustic radiation from the supersonic and subsonic regions of the jet. The over-all sound power level for the supersonic portion of the jet, W_A, is given by

$$W_A = \frac{10^{-4}}{9.6} m \frac{\rho_j}{\rho_a}\left(\frac{c_j}{c_a}\right)^5 c_j^2 M_j^{7-\alpha}(5M_j^2+0.8)\left(\frac{1+M_j^{\alpha-\beta}}{2}\right) \quad (1)$$

where ρ is the density, c the speed of sound, m the mass flow, and M is the Mach number. The subscripts j and a refer to the jet and ambient conditions respectively and α and β are exponents which depend on the type of nozzle and jet Mach number as discussed in Refs. 3 and 7. And the acoustic power from the subsonic portion of the jet, W_B, is given by

$$W_B = (10^{-4}/9.6)m(\rho_j/\rho_a)(c_j/c_a)^5 c_j^2 M_j^{7-\beta}[(5M_j^2+0.8)/5] \quad (2)$$

It was assumed in deriving this equation that the acoustic power output per unit length of the jet in the turbulent subsonic region

Table 2 Acoustic power levels for convergent nozzle, 191 tubes, 191 shrouds, and single shrouds

Configuration	L_w (db re 10^{-13} w)	Suppression Δdb
A. Outside air temp. ~ 20°F		
1. Press. ratio = 3.2, $M_j = 1.4$		
$1\frac{9}{16}$-in.-diam convergent nozzle	154.3	0
191 tubes	138.3	−16.0
Tubes, 6-in.-shrouds ($x_1 = \frac{3}{16}$ in.)	132.4	−21.9
Tubes, 6-in. shrouds ($x_1 = 1$ in.)	136.7	−17.6
Tubes, 6-in. shrouds ($x_1 = 2$ in., no induced flow)	135.5	−18.8
Tubes, S_{12}' shroud	138.7	−15.6
2. Press. ratio = 1.4, $M_j = 0.71$		
$1\frac{9}{16}$-in.-diam convergent nozzle	123.6	0
Tubes, 6-in. shrouds ($x_1 = \frac{3}{16}$ in.)	114.2	−9.4
B. Outside air temp. ~ 68°F		
1. Press. ratio = 3.2, $M_j = 1.4$		
$1\frac{9}{16}$-in.-diam convergent nozzle	150.7	0
191 tubes	135.5	−15.2
Tubes, 6-in. shrouds ($x_1 = \frac{3}{16}$ in.)	130.3	−20.4
Tubes, 3.335-in. shrouds ($x_1 = \frac{3}{16}$ in.)	131.7	−19.0
Tubes, 1.667 in. shrouds ($x_1 = \frac{3}{16}$ in.)	135.2	−15.5
Tubes, $S_{3.8}$ shroud	137.0	−13.7

decayed as x^{-6}. The total acoustic power output, W, from a supersonic jet exhaust is the sum of the power output from the supersonic region, Eq. (1), and the subsonic region, Eq. (2)

$$W = \frac{10^{-4}}{9.6} m \frac{\rho_j}{\rho_a}\left(\frac{c_j}{c_a}\right)^5 (c_j^2 M_j^7)(5M_j^2 + 0.8) \times \left[\frac{M_j^{-\alpha} + M_j^{-\beta}}{2} + \frac{M_j^{-\beta}}{5}\right] \quad (3)$$

Thus, the total acoustic power output from a supersonic jet is a function of the jet Mach number, density, and velocity of sound for both the jet and ambient gas.

Using the reservoir pressure of 46.4 psia and temperature of 73°F, and ambient pressure of 14.5 psia and temperature of 68°F in Eq. (1) the acoustic power output from the supersonic portion of the convergent nozzle was 72.2 w. The values of α and β used in Eq. (1) were 0.4 and -1.3, respectively as found in Ref. 7. For this acoustic power, the corresponding over-all sound power level is 148.6 db. The contribution from the subsonic portion of the jet from Eq. (2) was 18.4 w and the corresponding power level is 142.6 db. Thus, the total acoustic power from the convergent jet is 90.6 w and the corresponding over-all sound power level is 149.6 db. The over-all sound power level observed experimentally for the conditions used in the calculaton was 150.7 db as indicated in Table 2. This close agreement between theory and experiment was obtained because α and β were determined from the acoustic data for a 2-in.-diam convergent jet operated at a Mach number of 1.4.

For the same reservoir and ambient test conditions used in the analysis of the convergent nozzle, the mass flow through the 191 tubes was determined from an orifice meter to be 0.0586 slugs/sec. This mass flow is slightly less than that observed for the $1\frac{9}{16}$-in.-diam nozzle. By assuming that the 191 tubes can be considered as radiating acoustically without interference from each other and that the acoustic characteristics of a straight tube are similar to a convergent nozzle, the supersonic jet noise from each individual tube can be determined by the use of Eqs. (1–3). Thus, the acoustic power ouput from the supersonic region of 191 individual jets is 72.2 w, and 18.4 w from the subsonic region. For this assumed acoustic condition, the total acoustic power output from 191 tubes is 90.6 w with a corresponding over-all sound power level of 149.6 db. The experimentally observed over-all sound power level was 135.5 db for an ambient temperature of 68°F, Table 2. This difference in the calculated and experimental over-all sound power level is very large. Thus, the assumption of each of the 191 tubes radiating acoustically without interaction is not valid because of the large shielding effects of the supersonic jets from the multitubes.

In order to analyze the acoustic power output from the supersonic and subsonic regions for the multitubes, the Mach number distribution along the jet axis, as presented in Fig. 4, for the multitubes was used. It is apparent from this figure that the jet flow coalesces at approximately $1\frac{1}{2}$ in. from the tube exits. The coalesced flow behaves like a uniform subsonic jet at a Mach number of approximately 0.72 and remains nearly constant for about 4 diameters before decreasing as observed for subsonic jets in Ref. 7. Using the mass flow determined at 1 in. downstream of the multitubes from the radial surveys, the acoustic power output from this coalesced subsonic jet was calculated from the Lighthill equation

$$W = 10^{-4}(m/2)(\rho_j/\rho_a)(c_j/c_a)^5 c_j^2 M_j^7 \quad (4)$$

and the total power output was found to be 0.75 w with a corresponding sound power level of 128.8 db, which is less than the experimental value of 135.5 db, 3.55 w, for the multitubes at a Mach number of 1.4. Therefore, the acoustic radiation from the supersonic region is contributing to the over-all sound power output but not as great as the total of the individual radiation from the 191 tubes as discussed previously.

If it is assumed that only the outer ring of 52 tubes is radiating acoustically from the supersonic region to the outside, with the acoustic radiation from the inner tubes being shielded by the outer tubes, the calculated acoustic power output is 19.6 w and the corresponding power level is 142.9 db, which is much greater than the experimental value of 135.5 db. By assuming that only the outer 180° of each outer ring tube is radiating to the outside from the supersonic region, the acoustic power output is 9.83 w and the corresponding power level is 139.9 db, which is still greater than the experimentally observed value. The difference between the acoustic power calculated for the subsonic region by Eq. (2) and the experimental power is 2.80 w. For each tube the acoustic power output from the supersonic region is 0.377 w. Hence, it requires only 7.40 tubes to achieve 2.80 w, or approximately 51° from each of the outer rings of 52 tubes.

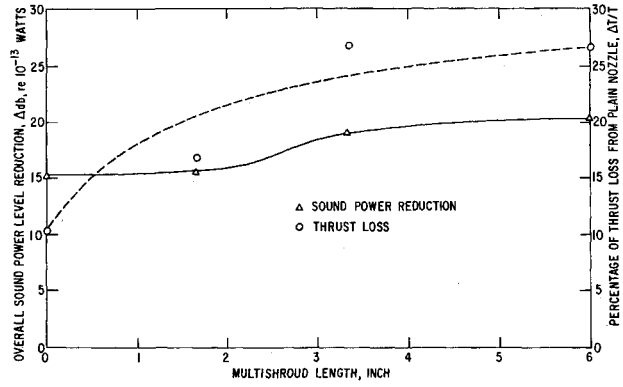

Fig. 12 Variation of over-all sound power level reduction and precentage thrust loss for 191 tubes with 191-shroud length.

It is evident from this initial analysis, with the assumptions used, that the shielding effects of the supersonic region from 191 tubes are extremely large. Only the equivalent of about 4.3% of the 191 tubes are radiating acoustic power from the supersonic region to the surrounding air.

The multitube concept is effective as a supersonic jet exhaust noise suppressor because of the following effects: 1) with the smaller diameter tubes in place of a single nozzle the supersonic region is decreased, supersonic region is proportional to the diameter and the jet Mach number as shown in Ref. 3; 2) because of the larger exposed surface of the primary jet flow to the ambient gas, the primary jet velocity is drastically decreased in a short distance and the coalesced jet acts like a subsonic uniform jet; 3) finally the most effective contribution to the noise reduction is the large attenuation of the acoustic waves through the supersonic region.

With the 191 tubes at a Mach number of 1.4, the thrust loss from an equivalent $1\frac{9}{16}$-in.-diam jet was 10.2% and the corresponding over-all sound power level reduction was 15.2 db. Thus, for this configuration the ratio of the sound power reduction to the thrust loss was 1.49. The decrease in the sound power level as well as the decrease in the thrust loss with the 1.667 in. multishrouds was slightly greater than for the multitubes alone as shown in Fig. 12. But for the 3.335 in. multishroud the over-all sound power level reduction was 19.0 db, Table 2, and the corresponding thrust loss was approximately 26%. By increasing the shroud length to 6 in. from 3.335 in., the over-all sound power level decreased 1.4 db compared to the shorter shroud with about the same thrust loss.

Conclusions

A supersonic jet noise suppressor consisting of 191 tubes and 191 hexagonal shrouds of various lengths was investigated at jet Mach numbers of 1.4 and 0.71. The effective area of 191 tubes of $\frac{1}{8}$ in. diam corresponds to a single $1\frac{9}{16}$-diam convergent jet. For a Mach number of 1.4, the location of the sonic Mach number on the axis was decreased from 19 in. to approximately 1 in. by the use of the 191 tubes. At $1\frac{1}{2}$ in. from the tube exit, the jets coalesced and the Mach number was 0.73 for 18 in. before

decreasing with axial distance. The over-all sound power level was decreased 15.2 db from the plain jet by the 191 tubes.

By adding the 191 hexagonal shrouds to the 191 tubes the Mach number at the shroud exits for shroud lengths of 3.335 and 6.0 in. was approximately 0.60 with the corresponding over-all sound power reductions of 19.0 and 20.4 db.

The peak impact pressure fluctuation was 4 mv at approximately 19 in. from the plain jet, which is close to the sonic location on the jet axis. With 191 tubes, the peak fluctuation was decreased to 1 mv at the 30 in. location and with the 3.335-in. multishrouds the peak fluctuations decreased to 0.6 mv at the 16 in. location. For all of the jet and suppressor configurations, the impact pressure fluctuations downstream of the peak location decreased as x^{-2}, which is characteristic of the fully developed subsonic turbulent jet decay region.

For a pressure ratio of 3.2 the power spectra for the 191 tubes was decreased approximately 25 db over the frequency range of 3000–5000 Hz from the plain convergent jet. Below and above this frequency range the decrease from the plain jet was not as great. The power spectra for the 3.335 and 6.0 in. multishrouds were quite similar with the greatest reduction from the plain jet occurring at 3500 Hz and for higher frequencies the reduction became less.

At a pressure ratio of 1.4 with corresponding jet Mach number of 0.71 the multitubes with 6.0 in. multishrouds decreased the over-all sound power level from the plain jet by 9.4 db.

References

[1] Nagamatsu, H. T., Sheer, R. E., Jr., and Wells, R. J., "Supersonic Jet Exhaust Noise Reduction with Rods, Shroud, and Induced Flow," *Proceedings of AFOSR-UTIAS Symposium on Aerodynamic Noise*, Toronto, May 20–21, 1968.

[2] Nagamatsu, H. T., Pettit, W. T., and Sheer, R. E., Jr., "Flow and Acoustic Measurements on a Convergent Nozzle Supersonic Jet Ejector," 69-C-156, April 1969, General Electric Research and Development Center, Schenectady, N.Y.

[3] Nagamatsu, H. T. and Horvay, G., "Supersonic Jet Noise," AIAA Paper 70-237, New York, 1970.

[4] Grande, E., "Possibilities and Devices for the Suppression of Jet Noise," Rept. D6-20609, Feb. 1968, Boeing Co.

[5] Coles, W. D. and Callaghan, E. E., "Full-Scale Investigation of Several Jet-Engine Noise-Reduction Nozzles," TN 3974, April 1959, NACA.

[6] Tatge, R. B. and Wells, R. J., "Model Jet Noise Study at Alplaus Facility," 61GL25, Jan. 1961, General Electric Co., Schenectady, N.Y.

[7] Nagamatsu, H. T., Sheer, R. E., Jr., and Gill, M. S., "Flow and Acoustic Characteristics of Subsonic and Supersonic Jets from Convergent Nozzle," CR-1693, Dec. 1970, NASA.

[8] Lighthill, M. J., "Jet Noise," *AIAA Journal*, Vol. 1, No. 7, July 1963, pp. 1507–1517.

[9] Nagamatsu, H. T., Sheer, R. E., Jr., and Gill, M. S., "Flow and Acoustic Characteristics of 191 Tubes and 191 Shrouds Supersonic Jet Noise Suppressor," AIAA Paper 71-153, New York, 1971.

MARCH 1972 AIAA JOURNAL VOL. 10, NO. 3

Heat Pipe Calorimetry for Plasma Stagnation-Point Heat Transfer

M. M. ABU-ROMIA* AND B. BHATIA†

Polytechnic Institute of Brooklyn, Brooklyn, N.Y.

The present investigation has the dual purpose of measuring stagnation-point heat-transfer rates in a jet produced by a commercial plasma torch, together with utilizing a heat pipe as a calorimeter for such measurements. In the experiment, the plane end of the cylindrical heat pipe was subjected to the plasma gas, and the heat received by the evaporator section of the pipe was measured by the change of the heat capacity of the cooling water at the condenser section. Heat-transfer results were obtained at plasma mean temperatures up to 12,000°K and at various gas flow rates to the torch. The data were compared with the theoretical laminar flow heat-transfer predictions, and good agreement is indicated for small mass flow rates to the torch. At large mass flow rates the plasma torch ceases to operate in the laminar regime, and as a result of the turbulence in the plasma jet the experimental heat-transfer results are much larger than what is predicted by the laminar theory.

Introduction

THE plasma torch, as one of several plasma generating devices available on the market today, has been utilized in several research and industrial applications such as welding, material testing and in studies of chemical synthesis. It is not surprising that many theoretical and experimental investigations dealing with the study of flow and temperature fields within the torch and within its plasma freejet have recently been reported.[1–4] It is the intent of this study to determine the heat-transfer rates to a plate placed normal to the torch axis and subjected to the high-temperature gas jet at various conditions of flow and power inputs to the torch. Prior to this investigation, it was not clear how these heat-transfer rates could be predicted for various flow regimes taking place within the torch, especially in view of the nonuniformity of temperature and velocity fields at the exit plane of the torch.

Several methods for measuring heat-transfer rates from high-temperature jets are available in the literature. They could be classified into transient and steady-state heat-transfer measurements.[5] Both methods have their shortcomings. For example, in the case of transient methods, difficulties arise due to the need to take into account the temperature dependence of the measuring sample. On the other hand, in the case of steady-state methods (which is often referred to as cooled-calorimeter method) errors associated with reverse flow of heat, which is not accounted for in the calorimetric computations, could become

Received January 20, 1971; presented as Paper 71-81 at the AIAA 9th Aerospace Sciences Meeting, New York, January 25–27, 1971; revision received October 29, 1971.

Index categories: Boundary Layers and Convective Heat Transfer—Laminar; Plasma Dynamics and MHD; Research Facilities and Instrumentation.

* Associate Professor, Department of Mechanical Engineering. Member AIAA.

† Graduate Student, Department of Mechanical Engineering.